

The petrosal and basicranial morphology of *Leptoreodon major* (Protoceratidae, Artiodactyla)

Selina Viktor Robson^{1,*}, Joshua A. Ludtke², Jessica M. Theodor¹

¹University of Calgary, Calgary, AB, T2N 1N4, Canada; selina.robson1@ucalgary.ca, jtheodor@ucalgary.ca

²MiraCosta College, 1 Barnard Dr, Oceanside, CA 92056, USA; jludtke@miracosta.edu

Abstract: *Leptoreodon* is a basal member of the Protoceratidae, an extinct group of artiodactyls variably allied with the Tylopoda and the Ruminantia. The basicranial morphology of other protoceratids (*Leptotragulus*, *Protoceras*, *Syndyoceras*) is similar to that of ruminants, supporting the hypothesis that the two clades are closely related. However, study of the basicranium of *Leptoreodon major* has revealed that protoceratid basicranial morphology is more variable than previously thought. *Leptoreodon* does share morphological features with some, if not all, other protoceratids, but the taxon also has some features not previously documented in the family, such as a deep subarcuate fossa. These previously undocumented features resemble the basicranial morphology of tylopods rather than ruminants, suggesting that previous hypotheses of protoceratid relationships need to be reexamined.

INTRODUCTION

The “Leptotragulinae” is a paraphyletic middle Eocene (Uintan and Duchesnean) radiation of bunoselenodont artiodactyls confined to North America (Wortman 1898; Scott 1899, 1940; Wilson 1974; Prothero 1998; Prothero and Ludtke 2007). Individual leptotraguline taxa have previously been referred to the Camelidae, Oreodontidae, Hypertragulidae, and Leptomerycidae (e.g., Wortman 1898; Matthew 1899; Peterson 1919; Gazin 1955; Stirton 1967), but leptotragulines are now considered to be basal protoceratids (Wilson 1974; Golz 1976; Black 1978; Prothero 1998; Prothero and Ludtke 2007). This referral is primarily based on dental characters, including a precocial derivation of selenodonty, a strong metaconid on the lower p₄, and strong lingual cingula on the upper molars (Wilson 1974). The two most abundant leptotraguline genera are *Leptotragulus* and *Leptoreodon*, but the subfamily also includes *Poabromylus*, *Toromeryx*, and *Heteromeryx* (Wilson 1974; Prothero 1998; Prothero and Ludtke 2007). Of these, *Leptotragulus* is thought to be the most basal taxon (Fig. 1) (Prothero, 1998).

The phylogenetic position of protoceratids remains a source of debate. Derived protoceratids have cranial appendages but such appendages are not present in leptotragulines (Patton and Taylor 1973). The dental and postcranial morphology of protoceratids resembles that of camelids and oromerycids, leading several researchers to refer the

Protoceratidae to the Tylopoda (Scott 1940; Gazin 1955; Stirton 1967; Wilson 1974; Golz 1976; Webb and Taylor, 1980; Webb 1981; Gentry and Hooker 1988; Prothero and Ludtke 2007). Conversely, the basicranial morphology of the derived protoceratid *Syndyoceras cooki* led Joeckel and Stavas (1996) to suggest that protoceratids are closely related to ruminants, rekindling a hypothesis from early studies of the family (Marsh 1891; Osborn and Wortman 1892; Scott 1895, 1899; Wortman 1898; Matthew 1905; Colbert 1941; Stirton 1944; Simpson 1945). Norris (2000) described the basicranium of *Leptotragulus* and agreed with Joeckel and Stavas (1996) that protoceratids resemble ruminants. Robson et al. (2021) recently described the basicranium of *Protoceras celer*, a protoceratid phylogenetically intermediate between *Leptotragulus* and *Syndyoceras* (Fig. 1). They concluded that many aspects of the basicranial morphology of protoceratids—such as a shallow subarcuate fossa and an endocranial ridge—is relatively conserved, but they identified some differences among *Protoceras*, *Leptotragulus*, and *Syndyoceras* (Robson et al. 2021). For example, *Protoceras* and *Syndyoceras* lack the rostral tympanic process of the petrosal found in *Leptotragulus*, but *Protoceras* retains a ventrally directed fenestra cochleae (Robson et al. 2021). These differences suggest that *Protoceras* represents a transitional morphology between basal and highly derived protoceratids (Robson et al. 2021).

The basicranial descriptions of *Protoceras* and *Syndyoceras* were based on computed tomography (CT) scans (Joeckel and Stavas 1996; Robson et al. 2021), but the descriptions

Published January 26, 2022

*corresponding author. © 2022 by the authors; submitted August 5, 2021; revisions received December 17, 2021; accepted December 18, 2021. Handling editor: Suzanne Cote. DOI 10.18435/vamp29378

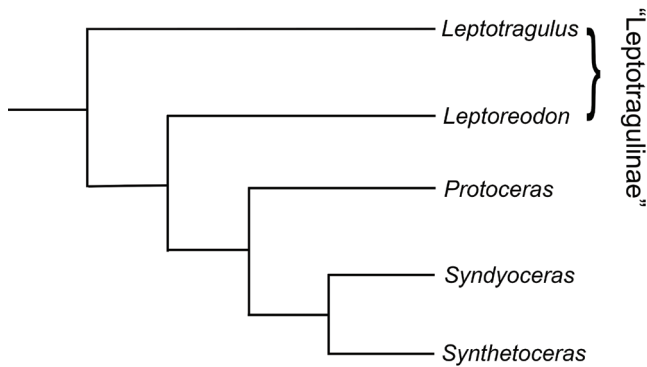


Figure 1. Hypothesized intrafamilial relationships of relevant Protoceratidae, based on Prothero (1998).

of *Leptotragulus* were based on physically dissected fossils (Norris 2000). Therefore, some morphological features, particularly the relationships among different skull bones, could not be documented. Until now, the study by Norris (2000) was the only published description of a leptotraguline basicranium, meaning that relatively little was known about the basicranial morphology of the group.

The basicranial morphology of leptotragulines is important because these taxa most likely represent the ancestral protoceratid condition, lending clues as to the phylogenetic position of the family. To build a more nearly complete dataset, we have CT-scanned and described the basicranium of *Leptoreodon*, a basal protoceratid inferred to be closely related to *Leptotragulus* based on shared morphology (Fig. 1; Prothero 1998). Both genera have characteristically strong upper molar lingual cingula and a short coronoid process on the mandible, only differing in some features of their p3 and p4 (Gazin 1955; Wilson 1974; Prothero 1998; Prothero and Ludtke 2007). Our description of the basicranium of *Leptoreodon* adds to our understanding of basal protoceratid morphology and documents early morphological variation within the family. These new data enable us to compare the basicranial morphology of *Leptoreodon* to that of *Leptotragulus*, *Protoceras*, and *Syndyoceras* to determine which features are conserved within basal protoceratids, and to examine whether basal protoceratids consistently have a basicranial morphology similar to the basicranial morphology of ruminants. We also describe the bony labyrinth morphology of *Leptoreodon* and compare it to that of other artiodactyls, including *Protoceras*.

MATERIALS AND METHODS

Institutional abbreviations

SDSNH, San Diego Natural History Museum, San Diego, CA, USA.

Material

SDSNH 47878 consists of a cranium with left C1-M3

and right C1-P1, a right dentary with p2-m3, a radius, ulna, scapula, atlas, and several vertebrae. The specimen is referred to *Leptoreodon major* (Ludtke and Prothero 2004). SDSNH 47878 was collected from the upper tongue of the Friar Formation, San Diego County, California, USA, and is of early Uintan (middle Eocene) age (Ludtke and Prothero 2004).

Computed tomography scan

SDSNH 47878 was subjected to micro-computed tomography (μ CT) scanning at the University of Calgary Micro-CT Laboratory. The specimen was scanned using a SkyScan 1173, operating at 130 kV and 61 μ A. The resultant scan was a stack of 990 images with voxel dimensions of 24.14 x 24.14 x 24.14 μ m.

The CT scan of SDSNH 47878 is available from MorphoSource.org under the project heading “*Leptoreodon major* basicranium” (<https://doi.org/10.17602/M2/M370397>). These data are freely available for download. The scan data were reconstructed using Amira 5.3 for Mac OS X (Visage, Inc., Chelmsford, MA: <http://www.visage.com>).

Measurements

We measured the basicranium and the bony labyrinths of SDSNH 47878, and we inferred body mass and agility scores based on these data. Straight line measurements (e.g., height, width) were taken using the built-in Amira 3D measurement tool, curved line measurements (e.g., semicircular canal length) were taken using the CreateSurfacePath function, and angles were taken using the 2D angle tools, the latter being used because all angles were measured in a single plane.

We measured the basicranial length (BL) of the specimen following the protocol outlined by Janis (1990). To estimate body mass, we used both the “all ungulates” and the “ruminants only” basicranial length regressions proposed by Janis (1990). We chose to use both equations because the phylogenetic position of protoceratids is ambiguous. The two body mass equations are:

$$\text{All ungulates: } \log_{10} BM (kg) = 3.137(\log_{10} BL) - 1.062$$

$$\text{Ruminants: } \log_{10} BM (kg) = 3.218(\log_{10} BL) - 1.209$$

We measured the height and width of the cochlea following Ekdale (2013) and calculated the aspect ratio of the cochlea using the associated Ekdale (2013) equation. We also approximated the length of the cochlear duct by measuring the length of the external cochlear coil. When possible, we measured the height and width of the semicircular canals following Spoor et al. (2007). We then used the Ekdale (2013) equation to compute the arc radius of each semicircular canal. We also measured the angles between the semicircular canals and the length of each semicircular canal.

We used the “all mammals” predictive equations proposed by Silcox et al. (2009) to estimate the agility score (AGIL) of *Leptoreodon*. Silcox et al. (2009) proposed separate agility equations for the anterior (ASCR), posterior (PSCR), and lateral (LSCR) semicircular canal radii, and an equation for the average semicircular canal radius (SCR); the semicircular canals of SDSNH 47878 were well-enough preserved that we were able to use all four equations. These predictive equations require that body mass be in grams.

$$\begin{aligned} \text{ASCR: } \log_{10} \text{AGIL} &= 0.850 - 0.153 (\log_{10} \text{BM}) + 0.796 (\log_{10} \text{ASCR}) \\ \text{PSCR: } \log_{10} \text{AGIL} &= 0.881 - 0.151 (\log_{10} \text{BM}) + 0.677 (\log_{10} \text{PSCR}) \\ \text{LSCR: } \log_{10} \text{AGIL} &= 0.959 - 0.167 (\log_{10} \text{BM}) + 0.854 (\log_{10} \text{LSCR}) \\ \text{SSCR: } \log_{10} \text{AGIL} &= 0.948 - 0.188 (\log_{10} \text{BM}) + 0.962 (\log_{10} \text{SSCR}) \end{aligned}$$

RESULTS

The CT scan of SDSNH 47878 captures the caudal portion of the skull (Fig. 2). The scan begins just rostral to the squamosal root of the zygomatic arch and terminates caudal to the occiput. The scan includes the entirety of the basicranium, excluding a portion of the occipital condyles that extend caudal to the occiput. There is some image distortion around the edges of the scan because of specimen movement during scanning. We take this distortion into account in our description. The rostral region of the scan includes unidentified bone fragments accreted onto the skull. We have not described these fragments as they are of unknown origin and do not pertain to the basicranial morphology of the specimen.

Petrosal

The petrosal of SDSNH 47878 is rostrocaudally elongate (Fig. 3). On the tympanic face, there is a rounded, hemi-ellipsoid promontorium (Fig. 3A, D). There are no transpromontorial or stapedial artery sulci present. An epitympanic wing projects anteriorly from the rostral edge of the promontorium. The ventral portion of the wing is rounded, whereas the dorsal portion of the wing forms a sharp, rostrally directed projection. The two parts of the wing are separated by a shallow concavity. We are unsure as to whether the dorsal, pointed part of the epitympanic wing is equivalent to the lateral process of the epitympanic wing as described by Orliac and O’Leary (2014). The epitympanic wing forms the sub-rectangular rostral border of the petrosal.

Ventrolaterally, the epitympanic wing is confluent with a downwards-projecting posteromedial flange that borders the base of the promontorium (Fig. 3A, D). The caudal edge of the posteromedial flange merges with the promontorium to form a rostral tympanic process. This process bulges caudally, abutting and defining the rostral rim of the fenestra cochleae. The fenestra cochleae is ventrocaudally

oriented whereas the fenestra vestibuli is laterally oriented.

The tympanic portion of the tegmen tympani roofs the epitympanic recess, which in turn is excavated by the fossa muscularis tensor tympani (Fig. 3A, D). A fossa for the head of the malleus is not present in the epitympanic recess. The secondary facial foramen is located at the caudal extent of the epitympanic recess, dorsal to the fenestra vestibuli. Dorsocaudal to the secondary facial foramen, the crista parotica originates from the lateral tegmen tympani and travels caudoventrally, bordering the stapedial muscle fossa and terminating at the stylomastoid notch, the petrosal contribution to the stylomastoid foramen. On the right side, the tympanohyal is fused with the petrosal and forms the lateral border of the stylomastoid foramen. The left tympanohyal is absent.

The tegmen tympani is triangular in dorsal view, coming to a point slightly caudal to the epitympanic wing (Fig. 3A, B, D). The tegmen tympani is relatively flat, moderately inflated, and lacks a tegmen tympani fossa (Orliac and O’Leary 2014). The hiatus Fallopii is a rostrally oriented slit-like hole on the lateral portion of the tegmen tympani, anterior to the epitympanic recess but posterior to the epitympanic wing (Fig. 3B). There is an apparent flange on the rostromedial portion of the tegmen tympani of the right petrosal, but no such structure is present on the left petrosal, suggesting that this “flange” may be a piece of broken bone that has been displaced from its original location.

The endocranial face contains the internal acoustic meatus and the subarcuate fossa (Fig. 3C). The area around the internal acoustic meatus is smooth. A prefacial commissure is present dorsal to the internal acoustic meatus, but there is no prefacial commissure fossa. Caudal to the prefacial commissure, the crista petrosa is a distinctive, thin rim dividing the tympanic face from the endocranial face. The subarcuate fossa appears to be elevated above the internal acoustic meatus because a ridge of bone separates the two structures, giving the endocranial face a stepped-like appearance. This ridge corresponds to a division between the cerebrum and cerebellum (Fig. 4). The distinction between the internal acoustic meatus and the subarcuate fossa is particularly pronounced at the ventral border of the subarcuate fossa where the ridge terminates in a rounded projection. The subarcuate fossa itself is shaped like a funnel; the diameter is relatively small, but the fossa is deep. There is an additional depression, identified as the mastoid fossa, at the bottom of the subarcuate fossa (Fig. 4C). There is no petromastoid canal.

A deep basicapsular groove [=petrobasilar canal (Norris, 2000)] runs along the ventromedial side of the petrosal, originating rostral to the internal acoustic meatus and terminating just rostral to the subarcuate fossa, at the

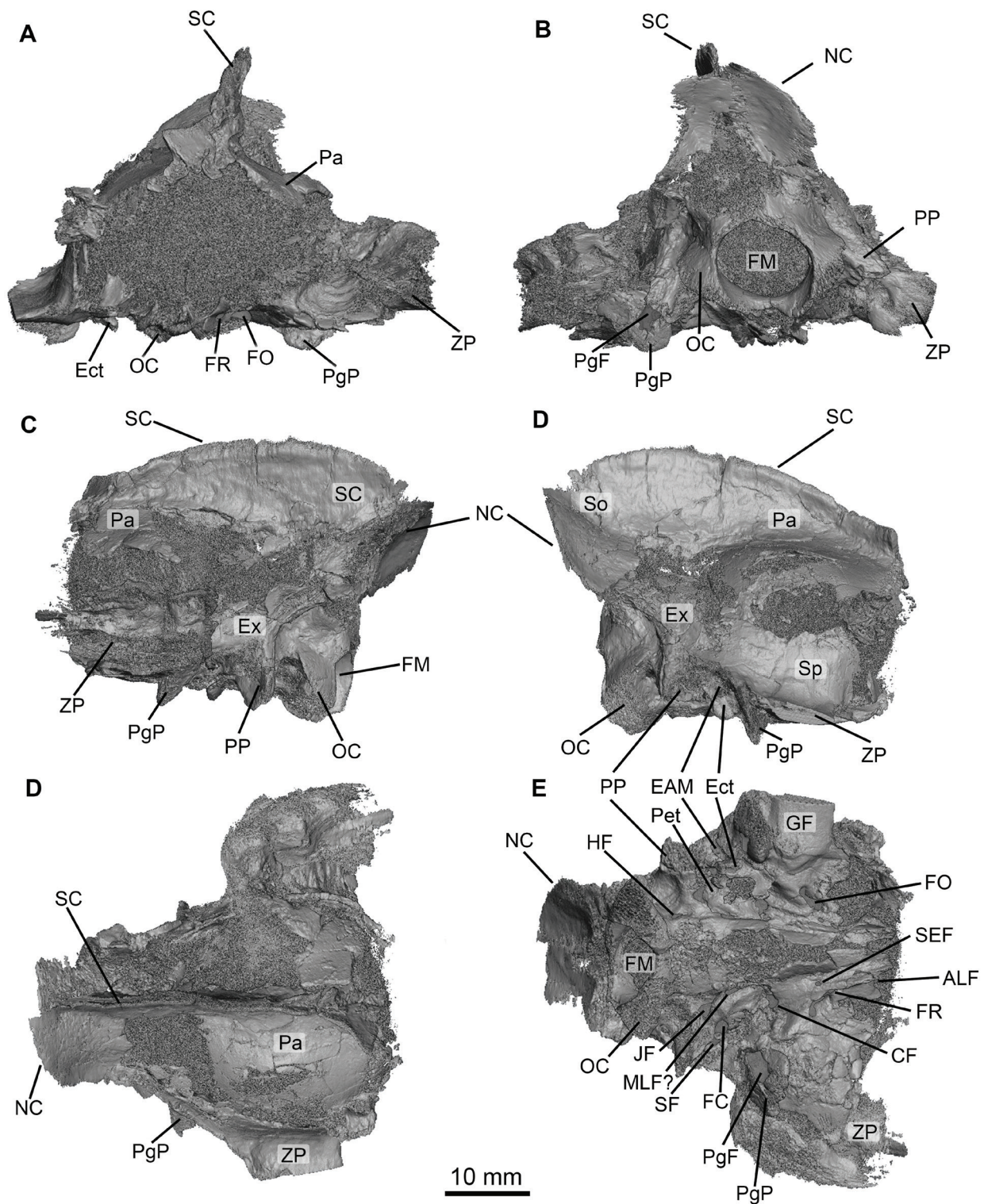


Figure 2. CT renderings of the basicranium of SDSNH 47878 in six orientations. Some features are outlined in black or shaded grey for emphasis. Junctions between bones are not outlined when the boundaries are indistinct. A, rostral view; B, caudal view; C, left lateral view, rostral direction left; D, right lateral view, rostral direction right; E, dorsal view, rostral direction right; F) ventral view, rostral direction right. Abbreviations: ALF, anterior lacerate foramen; CF, condylar foramen; EAM, external auditory meatus; Ect, ectotympanic; Ex, exoccipital; FC, fenestra cochleae; FM, foramen magnum; FO, foramen ovale; FR, foramen rotundum; GF, glenoid fossa; HF, hypoglossal foramen; JF, jugular foramen; MLF, middle lacerate foramen; NC, nuchal crest; OC, occipital condyle; Pa, parietal; Pet, petrosal; PgF, postglenoid foramen; PgP, postglenoid process; PP, paroccipital process; SC, sagittal crest; SEF, sphenoidal emissary foramen; SF, stylomastoid foramen; So, supraoccipital; Sq, squamosal; ZP, zygomatic process.

location of the afore described endocranial ridge (Fig. 3C). The vestibular aqueduct is located at the caudal end of the basicapsular groove. The cochlear aqueduct is located on the ventrolateral face of the petrosal, ventral to the internal acoustic meatus and the basicapsular groove (Fig. 3C, E).

The mastoid region of the petrosal is large, wedge shaped, and lacks a mastoid plate (Fig. 3) (O’Leary 2010). The relationship between the mastoid region and the surrounding bones cannot be determined because the external borders of the CT scan are indistinct. Based on published descriptions

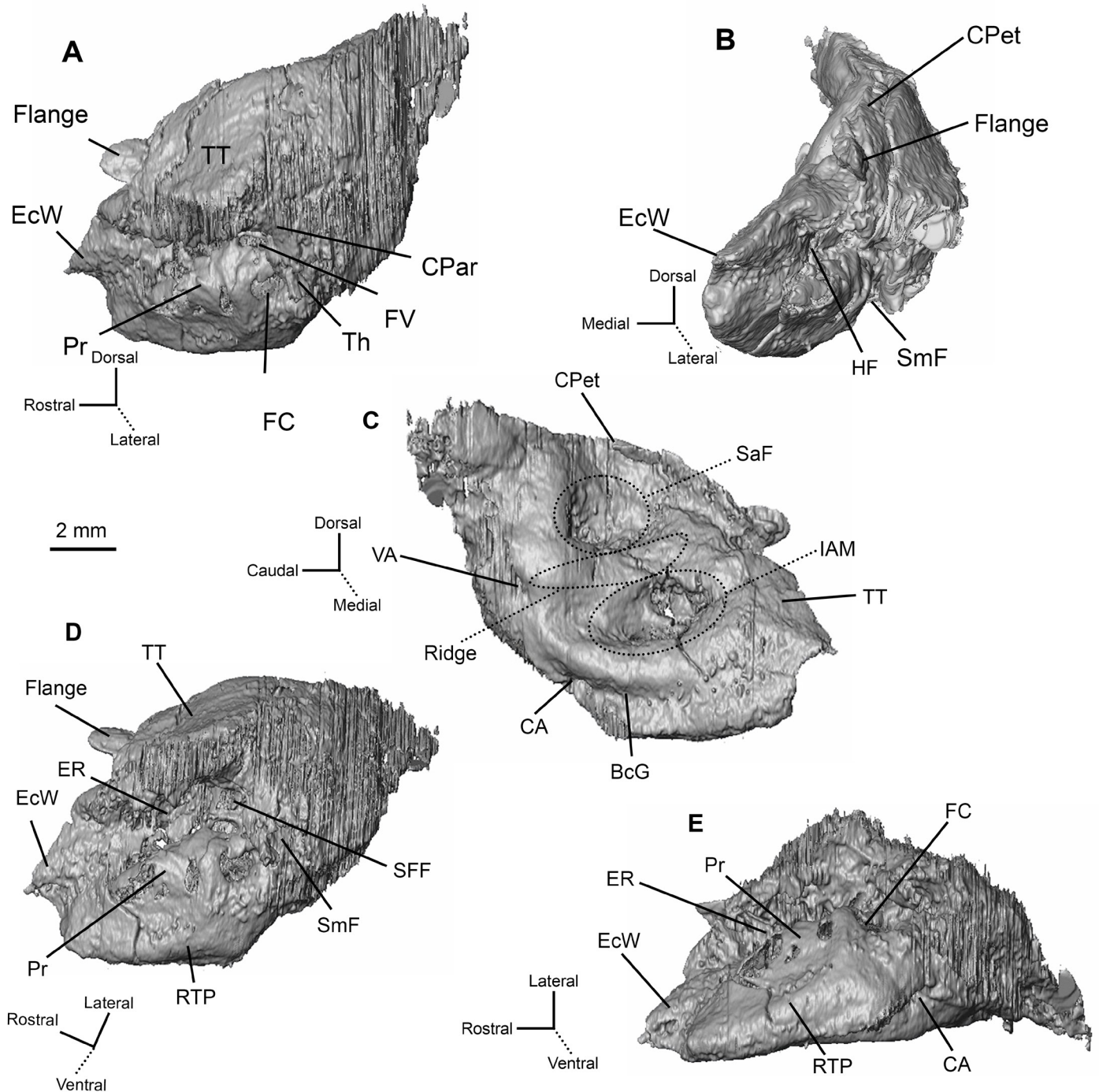


Figure 3. Five views of the right petrosal of SDSNH 47878. Images are mirrored so that the rostral direction is to the left of the image. A, lateral view; B, rostral view; C, endocranial (medial) view; D, tympanic view; E, ventral view. Abbreviations: BcG, basicapsular groove; CA, cochlear aqueduct; CPar, crista parotica; CPet, crista petrosa; EcW, ectotympanic wing; ER, ectotympanic recess; FC, fenestra cochleae; FV, fenestra vestibuli; HF, hiatus Fallopii; IAM, internal acoustic meatus; Pr, promontorium; RTP, rostral tympanic process; SaF, subarcuate fossa; SFF, secondary facial foramen; SmF, stylomastoid foramen; Th, tympanohyal; TT, tegmen tympani; VA, vestibular aqueduct.

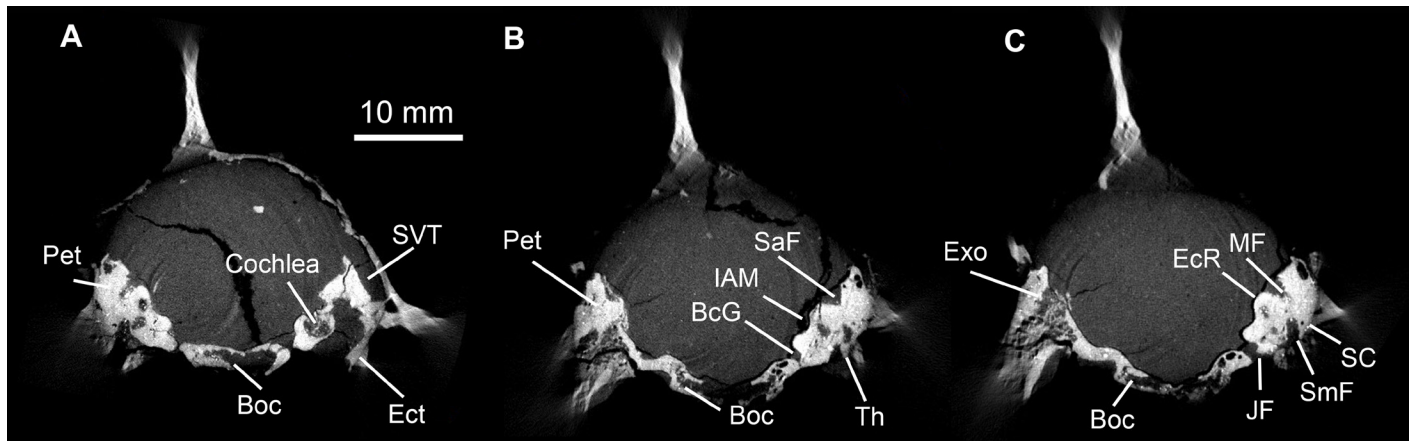


Figure 4. Transverse CT slices of SDSNH 47878. Higher numbered slices are located more rostrally. A, slice 101; B, slice 906; C, slice 875. Abbreviations: BcG, basicapsular groove; Boc, basioccipital; EcR, endocranial ridge; Ect, ectotympanic; Exo, exoccipital; IAM, internal acoustic meatus; JF, jugular foramen; MF, mastoid fossa; Pet, petrosal; SaF, subarcuate fossa; SmF, stylomastoid foramen; SC, semicircular canal; SVT, sinus venosus temporalis; Th, tympanohyal.

of *Leptoreodon* (= *Camelomeryx*), the mastoid region of the petrosal is visible externally (i.e., the mastoid condition) between the squamosal and the exoccipital (Scott 1899).

Bony labyrinth

Partial bony labyrinths of both ears are preserved. The left bony labyrinth is more nearly complete and is the primary basis of this description (Fig. 5). The cochlear canal makes approximately 2.5 turns (rotation of 900°). The vestibule, consisting of the saccule (spherical recess) and utricle (elliptical recess), could be partially reconstructed, but the shape is indistinct because of poor preservation. The vestibular aqueduct is a long and narrow channel that originates from the medial side of the common crus. The cochlear aqueduct is shorter than the vestibular aqueduct, but the two channels are approximately equal in diameter.

All three semicircular canals are present in the specimen. Both the anterior and posterior semicircular canals extend dorsally above the common crus, forming a distinct V-shape. Of these, the anterior semicircular canal has the greatest dorsal extent. The posterior and lateral semicircular canals are straight, but the anterior semicircular canal is slightly sinusoidal, curving medially from the common crus and then laterally toward the anterior ampulla. The anterior ampulla is situated slightly more dorsally than the lateral and posterior ampullae; the latter two lie in approximately the same plane. All three ampullae are bulbous. There is no secondary common crus, but the paths of the posterior and lateral semicircular canals do overlap as they enter the posterior ampulla.

Of the three canals, the anterior semicircular canal has the greatest radius, and the lateral semicircular canal has the smallest radius (Tab. 1). The lateral semicircular canal is much wider than it is high, resulting in the canal having an oval rather than circular appearance. The angle between the

anterior and posterior semicircular canals is the smallest, and the angle between the posterior and lateral semicircular canals is the largest (Tab. 1). The angle formed between the posterior and lateral canals is the only one larger than 90°.

Ectotympanic

The left ectotympanic is missing, but a partial right ectotympanic is present (Fig. 2E). The lateral portion of the ectotympanic forms a triangular plate and comprises the ventral and rostral borders of the external auditory meatus. The ectotympanic curves rostromedially past the external auditory meatus but, if a styloid process was present, it is now missing. Not enough of the ectotympanic is present to determine the complete internal composition. The remnants of the ectotympanic are curved in a way that suggests a hollow chamber may have been contained within the bone when it was whole. The present portions of the ectotympanic are dense and, even with potential artifacts from scan movement, it is unlikely that the ectotympanic was composed of cancellous bone (Fig. 4A).

Squamosal

Most of the squamosal morphology was captured in the scan, including the root of the zygomatic arch and the glenoid fossa (Fig. 2). The lateral extent of the zygomatic arches was not captured because it was outside of the frame of the scan window. The zygomatic arch is rostrocaudally broad, and the medial half of the glenoid fossa is very gently convex. A small, rounded, and pneumatized postglenoid process borders the caudal edge of the glenoid fossa (Fig. 2C–E). This postglenoid process contacts the ectotympanic, but it does not appear to form any part of the external auditory meatus. A very large postglenoid foramen pierces the caudal wall of the postglenoid process—the foramen occupies at least half of the caudal wall as well as the area directly posterior to the process, encroaching on the ecto-

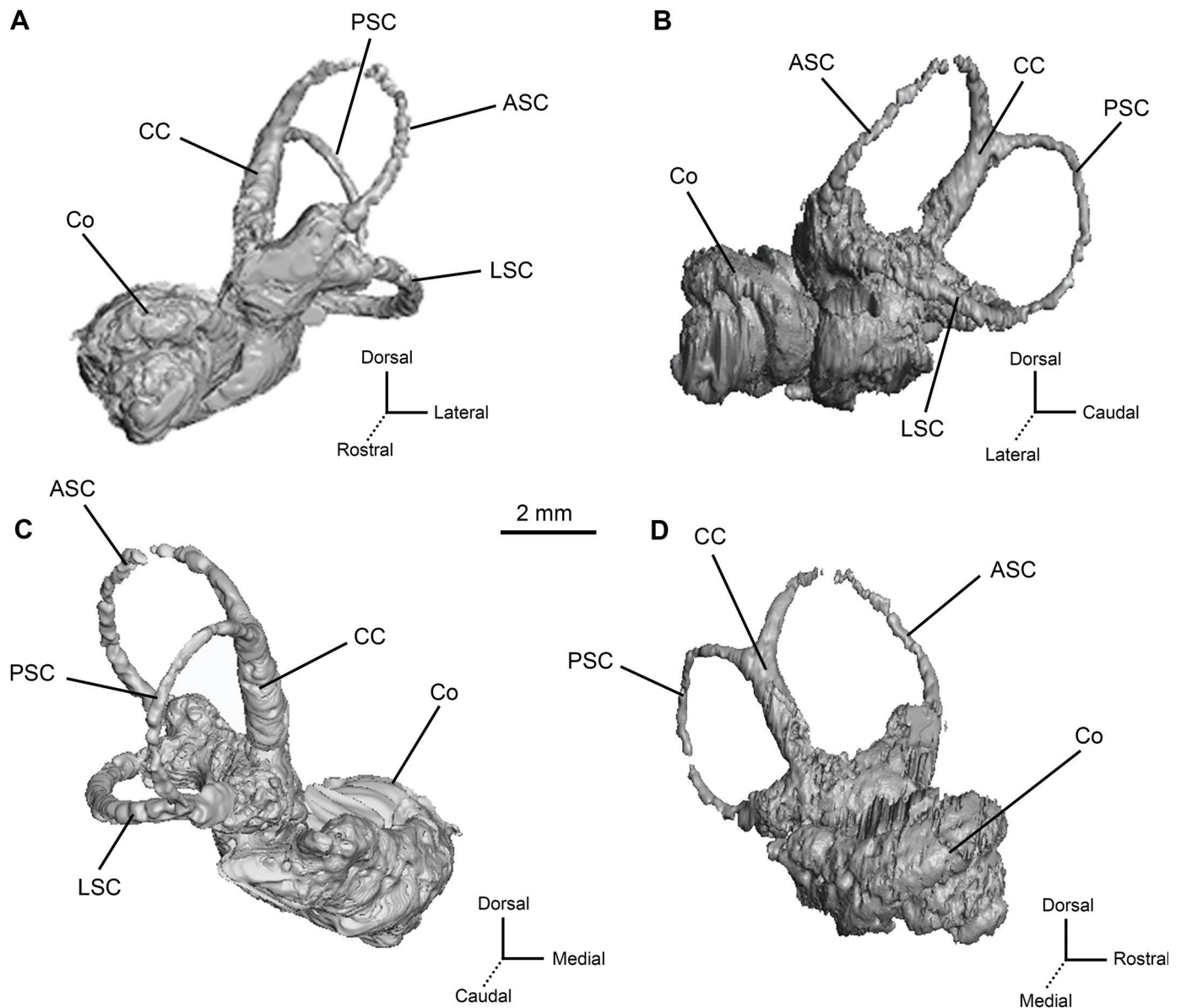


Figure 5. Four views of the left bony labyrinth of SDSNH 47878. A, rostral view; B, lateral view; C, caudal view; D, medial view. Abbreviations: ASC, anterior semicircular canal; CC, common crus; Co, cochlea; LSC, lateral semicircular canal; PSC, posterior semicircular canal.

tympanic (Fig. 2E). The left postglenoid foramen may be artificially enlarged because of breakage, but the intact right postglenoid foramen still occupies a large portion of the postglenoid process and encroaches on the ectotympanic. Internally, this foramen joins with a large sinus venosus temporalis (Fig. 4A). A post-tympanic process could not be identified on the specimen.

Parietal

The dorsal portion of the parietals were preserved on the specimen (Fig. 2). SDSNH 47878 has a thin but pronounced sagittal crest that originates above the glenoid fossa and extends caudally to the occiput. The sagittal crest bifurcates rostrally, forming two smaller, rostromedially

trending crests. Only the caudal extent of these crests is captured in the frame of the scan window. The lateral morphology of the parietals cannot be described as both sides are poorly preserved.

Supraoccipital

Fragments of the supraoccipital are present (Fig. 2). The most prominent feature of the supraoccipital is the flared, bilateral nuchal crests that define the occiput. The dorsal and lateral edges of the nuchal crest were not preserved, but even with the breakage, the crest is quite pronounced on both sides of the specimen. The crest curves slightly downwards as it extends laterally, giving the occiput a concave shape.

Table 1. Measurements of SDSNH 47878, and body masses and agility scores inferred based on those measurements. Length measurements are in mm and mass measurements are in kg. Agility scores are unitless. Abbreviations: AGIL, agility score; ASC, anterior semicircular canal; h, height; l, length; LSC, lateral semicircular canal; PSC, posterior semicircular canal, w, width.

Basicranial length 37.58		
	Left	Right
ASC h	3.90	--
ASC w	3.65	3.58
ASC l	7.06	--
ASC arc radius	1.89	--
PSC h	3.11	3.42
PSC w	3.00	3.54
PSC l	5.80	--
PSC arc radius	1.53	1.74
LSC h	2.17	2.55
LSC w	3.11	3.09
LSC l	5.31	--
LSC arc radius	1.32	1.41
Angle ASC/PSC	76.4°	75.8°
Angle ASC/LSC	83.8°	89.6°
Angle PSC/LSC	95.7°	95.5°
Cochlea h	3.18	--
Cochlea w	3.98	--
Cochlea coil l	22.22	--
Cochlea aspect ratio	0.80	--
ASC AGIL (ruminants only)	3.03	--
ASC AGIL (all artiodactyls)	2.97	--
PSC AGIL (ruminants only)	2.76	3.08
PSC AGIL (all artiodactyls)	2.76	3.01
LSC AGIL (ruminants only)	2.80	2.97
LSC AGIL (all artiodactyls)	2.74	2.89
SSC AGIL (ruminants only)	2.85	--
SSC AGIL (all artiodactyls)	2.72	--

Exoccipital

The junctions between the exoccipital and the surrounding bones are indistinct (Fig. 2). However, the exoccipital clearly has a pronounced paroccipital process that carries the nuchal crest along its lateral surface. The tip of the process is missing, but the base of the process projects ventrolaterally and quickly becomes rostrocaudally flattened. The caudoventral base of the process forms a convex fossa (Fig. 2E).

Basioccipital

The basioccipital defines the ventral border of the foramen magnum (Fig. 2). The rostral part of the bone is thin with some ventral pneumatization (Fig. 4). The frame of the CT scan window only captured the rostral portion of the occipital condyles, which extend from the exoccipitals to the basioccipital. The ventral surface of the condyles is broken off, exposing the internal pneumatization. There is a rostrally-directed bilateral groove that runs from the base of the occipital condyles along the lateral sides of the basioccipital (Fig. 2E). The hypoglossal foramen is located on the lateral aspect of the bone, just rostral to the condyles, at the caudal end of this groove (Fig. 2E). More rostrally, there is a gap between the basioccipital and the medial petrosal, likely either the middle lacerate foramen or part of the basicapsular fissure (see O'Leary (2016) for definition; Fig. 2E). There is also a medial groove that extends from the foramen magnum towards the basisphenoid.

Internally, the dorsolateral surface of the basioccipital contacts the ventromedial edge of the petrosal. When in contact, the basioccipital makes a minor contribution to the ventral border of the basicapsular groove, a channel primarily located on the petrosal (Fig. 4B). The contact between the basioccipital and the petrosal is interrupted caudally by the jugular foramen (Fig. 4C). The jugular foramen is the exit for the inferior petrosal sinus, which is the soft tissue structure most likely carried by the basicapsular groove. The basicapsular groove is not present caudal to the jugular foramen. Rostrally, the basioccipital and petrosal remain closely associated with only a small gap between them (Fig. 4A). However, the basicapsular groove becomes less pronounced once the bones lose direct contact.

Basisphenoid

The basisphenoid sits rostral to the basioccipital (Fig. 2). The medial section of the basisphenoid is broken; therefore, it is unclear whether the medial groove of the basioccipital continues onto the basisphenoid. However, the paired lateral grooves that originated on the basioccipital are present on the basisphenoid. The carotid foramen is located at the caudolateral end of the bone; the basisphenoid defines the rostral edge of the foramen while the petrosal and ectotympanic define the rest (Fig. 2E). Rostrolaterally, there is a massive, oval-shaped foramen ovale (Fig. 2A, E). The lateral wall of the foramen ovale is formed by the squamosal. Rostral to the foramen ovale, located entirely on the basisphenoid, is a circular foramen rotundum. On the right side of the specimen, there are two equally sized foramina in this position. These foramina may represent a duplication of the foramen rotundum. An anteriorly directed ridge, potentially part of the pterygoid process, originates ventral to the foramen ovale (Fig. 2E). On the

left side, at the base of this ridge and medial to the foramen ovale, another small foramen is present. We interpret this to be the sphenoidal emissary foramen. Two small foramina sit rostral to the foramen rotundum on the left side. These foramina are at the anterior margin of the CT scan. One, if not both, of these foramina likely represent the anterior lacerate foramen.

Body mass and agility scores

The basicranial length of SDSNH 47878 is 37.58 mm. Based on this measurement, the body mass of the specimen is estimated to be either 4.76 kg, derived from the “ruminants only” regression equation, or 5.52 kg, derived from the “all ungulates” regression equation (Tab. 1).

Agility scores were calculated based on the arc radius of each semicircular canal and the average arc radius of all three the semicircular canals. Agility scores range from 2.72 to 3.08, depending on which semicircular canal and body mass estimate is used (Tab. 1). The body mass predicted by the “ruminants only” regression is larger and therefore produces slightly higher agility score estimates. The arc radii of the right semicircular canals are also slightly larger than the arc radii of the left canals, resulting in higher agility scores. Such variation is known to occur in other ungulates as is likely the result of true variation within the individual rather than an artifact of taphonomy or CT scanning (Danilo et al. 2015: supplemental information).

DISCUSSION

Descriptions of material referred to *Leptoreodon* have focused on the dentition and postcrania (Stock 1936; Gazin 1955; Wilson 1974, 1984; Golz 1976; Kelly 1990; Ludtke and Prothero 2004). Wortman (1898) and Scott (1898) offered brief overviews of the skull, but the only detailed cranial description was provided by Scott (1899), who published specimens of *Leptoreodon* under the junior synonyms *Merycodesmus gracilis* and *Camelomeryx longiceps* (Gazin 1955). As such, there are few published descriptions of *Leptoreodon* basicrania. However, other protoceratid genera have been described in much greater detail, presenting an opportunity for comparison.

Petrosal

The petrosal of *Leptoreodon* exhibits a combination of ancestral and derived features. Like *Leptotragulus*, another basal protoceratid, *Leptoreodon* has a large rostral tympanic process that encroaches on the fenestra cochleae (Norris 2000). Norris (2000) suggested that the great size of the rostral tympanic process may have forced the fenestra cochleae of *Leptotragulus* to be ventrally oriented—we have observed a similar effect in *Leptoreodon*, where the fenestra cochleae has a distinctly ventrocaudal orientation.

Norris (2000) noted that an equally large rostral tympanic process is present in basal ruminants and suggested that this may be a shared morphology uniting the two groups. The presence of a large rostral tympanic process in both *Leptotragulus* and *Leptoreodon* does suggest that this is the ancestral morphology for protoceratids. The relatively derived protoceratid *Protoceras* does not have an enlarged rostral tympanic process, but the fenestra cochleae is still ventrocaudally oriented, perhaps a holdover from the ancestral condition (Robson et al. 2021).

In *Leptoreodon*, the epitympanic wing of the petrosal has two parts, a rounded ventral portion and a dorsal pointed portion. This latter portion may be the lateral process of the epitympanic wing. When present, the lateral process forms the caudolateral border of the piriform fenestra (Orliac and O’Leary 2014). We could not locate the piriform fenestra in SDSNH 47878. Rather, the dorsal portion of the epitympanic wing defines the caudolateral border of a large foramen we identified as the carotid foramen. It is possible that the piriform fenestra and the carotid foramen are merged in the specimen or that the division between the two was not preserved. *Protoceras* has a similar morphology, although the pointed dorsal portion of the epitympanic wing is not quite as pronounced (Robson et al. 2021). Conversely, Norris (2000) did not describe or figure a lateral process on *Leptotragulus*, and the rostral border of the *Leptotragulus* petrosal appears to be fully rounded. A comparison between protoceratids and other artiodactyls with a lateral process may resolve the identity of the process, but regardless, there does appear to be variation in epitympanic wing morphology within the Protoceratidae.

Despite being visible externally (i.e., the mastoid condition; Scott 1899), the *Leptoreodon* petrosal lacks a mastoid process. This is in direct contrast to *Protoceras*, which has a massive mastoid process that forms the externally visible portion of the petrosal (Robson et al. 2021). *Leptotragulus* also lacks a large mastoid process (Norris 2000), suggesting that the *Protoceras* condition is derived. However, given that both *Leptotragulus* and *Leptoreodon* have the mastoid condition, it is likely that mastoid exposure is the ancestral condition for protoceratids.

There is also intrafamilial variation in the presence of a tegmen tympani fossa, a depression on the tegmen tympani that may have received part of the temporal lobe of the cerebrum and the trigeminal ganglion (Orliac and O’Leary 2014). *Leptoreodon* does not have a tegmen tympani fossa, and it is not known whether *Leptotragulus* has one. A tegmen tympani fossa is present in *Protoceras* (Robson et al. 2021) and potentially in *Syndyoceras* (Joeckel and Stavas 1996), although its presence in the latter cannot currently be confirmed. Robson et al. (2021) suggested that the morphology observed in *Protoceras* may be a transitional

state between the ancestral condition and the highly derived morphology of *Syndyoceras*; *Syndyoceras* has a rostromedial shelf-like process that forms a groove which may have transmitted the trigeminal nerve or ganglion (Joeckel and Stavas 1996). Given that *Leptoreodon* does not have a tegmen tympani fossa, it is quite possible that *Protoceras* is exhibiting a derived condition. Examination of other derived protoceratids is necessary to determine the distribution within the family and to determine if the morphology of *Protoceras* is indeed a transitional state.

Like other protoceratids, *Leptoreodon* has a distinct endocranial ridge separating the cerebral and cerebellar faces of the petrosal (Joeckel and Stavas 1996; Norris 2000; Robson et al. 2021), a morphology that has previously been argued to ally protoceratids with ruminants (Joeckel and Stavas 1996; Norris 2000). The presence of such a ridge in both *Leptotragulus* and *Leptoreodon*, two of the most basal protoceratids, strongly suggests that this is the ancestral morphology of the family. A similar ridge is present in several extant ruminants (Norris 2000), but its distribution among extinct ruminants has yet to be documented. *Poebrotherium*, a basal camelid, and anoplotheriids, a family of extinct endemic European artiodactyls, also appear to have this morphology (Dechaseaux 1969; Norris 2000; O'Leary 2010; Orliac et al. 2017), and an endocranial ridge may be more common in artiodactyls than is currently known.

Leptoreodon, like *Leptotragulus* and *Syndyoceras*, lacks a petromastoid canal (Joeckel and Stavas 1996; Norris 2000). *Protoceras* has a petromastoid canal, which Robson et al. (2021) suggested was either a retention of the ancestral condition or an independent derivation of the feature. The absence of a petromastoid canal in *Leptoreodon* supports the latter interpretation; *Protoceras* likely evolved a petromastoid canal independently.

One of the most striking differences between *Leptoreodon* and other protoceratids is the presence of a deep subarcuate fossa in *Leptoreodon*—the subarcuate fossa of *Leptotragulus*, *Protoceras*, and *Syndyoceras* is a shallow depression (Joeckel and Stavas 1996; Norris 2000; Robson et al. 2021). Pecoran ruminants also have a shallow subarcuate fossa, and similarities between the protoceratid and ruminant subarcuate fossa have been suggested to unite the two clades (Joeckel and Stavas 1996; Norris 2000). Conversely, most camelids have a deep subarcuate fossa (Whitmore 1953; Joeckel and Stavas 1996; O'Leary 2010). A shallow subarcuate fossa was considered to be the ancestral protoceratid condition because *Leptotragulus* has a shallow subarcuate fossa (Norris 2000). *Leptoreodon* demonstrates that protoceratid subarcuate fossa morphology is more variable than previously thought, and the presence of a deep subarcuate fossa in *Leptoreodon* renders the ancestral protoceratid condition ambiguous. It is possible that

Leptoreodon independently derived a deep subarcuate fossa, but it is also possible that multiple protoceratids derived a shallow subarcuate fossa. The basal camelid *Poebrotherium*, which has been hypothesized to be closely related to the protoceratids (e.g., Patton and Taylor 1971, 1973; Gentry and Hooker 1988), has a deep subarcuate fossa similar in shape to that of *Leptoreodon* (O'Leary 2010).

Systematics arguments based on subarcuate fossa morphology are further called into question by the presence of a mastoid fossa in *Leptoreodon*. The mastoid fossa is a depression in the subarcuate fossa that, in life, housed the lobulus petrosus of the cerebellum (Whitmore 1953). The absence of a mastoid fossa is another character that has been used to ally protoceratids with ruminants to the exclusion of camelids (Joeckel and Stavas 1996; Norris 2000), the latter being one of the few artiodactyl families known to possess such a fossa (Whitmore 1953; Joeckel and Stavas 1996; Norris 2000). Considering that *Leptoreodon* has both a deep subarcuate fossa and a mastoid fossa, the argument for a relationship between protoceratids and ruminants based on subarcuate fossa morphology requires reexamination.

Bony labyrinth

The only other described protoceratid bony labyrinth is that of *Protoceras* (Robson et al. 2021). Based on this description, *Leptoreodon* and *Protoceras* have a similar bony labyrinth morphology. Both taxa share a vestibular aqueduct and cochlear aqueduct morphology that is typical of artiodactyls (e.g., Orliac et al. 2012, 2017; Mennecart and Costeur 2016a). Only the anterior semicircular canal was present in the described *Protoceras* specimen, but in both taxa, the anterior semicircular canal has a similar shape and lies in more than one plane (Robson et al. 2021).

The two taxa also have a similar cochlea. The *Protoceras* cochlea has 2.75 turns whereas the *Leptoreodon* cochlea has 2.5 turns (Robson et al. 2021). Intrafamilial variation in cochlear coiling can occur, typically within a range of 0.5 turns (Mennecart and Costeur 2016a, b), and *Leptoreodon* and *Protoceras* are well-within this range. The cochlear turns of *Leptotragulus* are within the ranges reported for bovids (2.5), cervids (2.25–2.5), and moschids (2.5) (Costeur 2014; Mennecart et al. 2016), whereas those of *Protoceras* are more similar to tragulids (Robson et al. 2021). However, few bovids and moschids have been sampled, and it is possible that other taxa within those families have a larger number of cochlear turns.

The *Leptoreodon* cochlea has an aspect ratio of 0.80, which is identical to the aspect ratio of the *Protoceras* cochlea (Robson et al. 2021). Protoceratids have the highest known cochlear aspect ratio of any artiodactyl, although other artiodactyl taxa, such as the anoplotheriid *Diplobune minor*, do reach aspect ratios above 0.70 (Ekdale 2009; Mennecart

and Costeur 2016b; Orliac et al. 2017). Ruminants are known to have a cochlear aspect ratio ranging from 0.52–0.68 (Costeur 2014; Mennecart et al. 2016), although there are several ruminant families that have not been sampled. The aspect ratio of camelids is not known. It seems that a high cochlear aspect ratio was evolved early within the Protoceratidae and remained present in at least some derived taxa. To our knowledge, a high cochlear aspect ratio does not have any clear functional implications, but cochlear aspect ratios have been hypothesized to be phylogenetically significant (Ekdale 2013). Overall, bony labyrinth morphology appears to be conserved within the family, although more protoceratid taxa should be sampled.

Ectotympanic

To our knowledge, a description of a complete *Leptoreodon* ectotympanic has never been published. Indeed, there do not appear to be published descriptions of any leptotraguline auditory bullae (Norris 2000). Scott (1899) noted that none of the *Leptoreodon* specimens he studied had an ectotympanic, but he inferred that the ectotympanic and external auditory meatus were quite small. This is compatible with observations of derived protoceratids, which have small, uninflated, and hollow bullae (Scott 1895, 1940; Patton and Taylor 1973; Joeckel and Stavas 1996). Based on SDSNH 47878, the external auditory meatus of *Leptoreodon* is not unusually small, but we cannot comment on the size of the ectotympanic because the bone is incomplete. The partial ectotympanic does appear to have been hollow, which would suggest that protoceratids retained a hollow auditory bulla throughout their evolution. The lateral portion of the *Leptoreodon* ectotympanic contributes to the rostral and ventral borders of the external auditory meatus, a condition also present in *Protoceras* (Robson et al. 2021) and further evidence that protoceratid ectotympanic morphology is conserved within the family.

Squamosal

Like the petrosal, the squamosal of *Leptoreodon* possesses a combination of ancestral and derived morphologies. The glenoid fossa of *Leptoreodon* appears to be flatter than that of other protoceratids (Scott 1895; Patton and Taylor 1971, 1973; Robson et al. 2021), although it is possible this is a result of poor preservation or scanning distortion. Norris (2000:343) described the glenoid fossa of *Leptotragulus* as “gently convex,” and Scott (1899:71) described the glenoid fossa of *Leptoreodon* (= *Camelomeryx*) as “broad and simply convex,” which suggests that the convexity of the leptotraguline glenoid fossa is typically minor.

Unlike *Protoceras*, the postglenoid process of *Leptoreodon* is pneumatized (Robson et al. 2021). The condition of other protoceratids is not currently known, so it is unclear

whether pneumatization is common among protoceratids. Protoceratids, including *Leptoreodon*, have a postglenoid foramen that penetrates the postglenoid process (Joeckel and Stavas 1996; Norris 2000; Robson et al. 2021). Joeckel and Stavas (1996) noted that this is a derived condition among artiodactyls, a result of auditory region compression as the postglenoid process and post-tympanic process move closer together. Scott (1899) described the presence of a distinct post-tympanic process in *Leptoreodon* (= *Camelomeryx*), but the *Leptoreodon* specimen illustrated by Wortman (1898) does not appear to possess such a process, and we could not locate a post-tympanic process on SDSNH 47878. We cannot determine if this discrepancy is the result of intrageneric variation or specimen breakage without a more extensive examination of specimens referred to *Leptoreodon*. Other protoceratid taxa have a post-tympanic process (Scott 1895; Patton and Taylor 1971, 1973; Joeckel and Stavas 1996; Norris 2000; Robson et al. 2021) and, to our knowledge, the absence of a post-tympanic process is unusual among artiodactyls.

Protoceratids consistently have a sinus venosus temporalis (Joeckel and Stavas 1996; Norris 2000; Robson et al. 2021). The sinus venosus temporalis of *Leptotragulus* and *Protoceras* is larger than that of *Syndyoceras* (Norris 2000; Robson et al. 2021). There are no published images of the *Leptotragulus* sinus venosus temporalis, so direct comparisons to that taxon cannot be made. However, the sinus venosus temporalis of *Leptoreodon* is larger than that of *Protoceras* (Robson et al. 2021), approaching the size observed in *Merycoidodon* and *Poebrotherium*, although the sinus venosus temporalis of *Leptoreodon* never reaches the same medial extent as it does in those taxa (Whitmore 1953). The larger size of the sinus venosus temporalis in *Leptoreodon* compared to *Protoceras* and *Syndyoceras* suggests that the structure became reduced over time within the family.

Parietal, supraoccipital, and exoccipital

The cranial roof of SDSNH 47878 matches previous descriptions and illustrations of *Leptoreodon* (Wortman 1898; Scott 1899). This includes a pronounced sagittal crest and a nuchal crest that extends onto the paroccipital process of the exoccipital. *Leptoreodon* also has a semi-circular, arched supraoccipital region, caused by the expansion of the nuchal crests, which is characteristic of protoceratids (Patton and Taylor 1971, 1973; Norris 2000).

Basioccipital

Protoceratids typically have a basioccipital marked by a rostrally-directed median groove (Scott 1940; Joeckel and Stavas 1996; Norris 2000; Robson et al. 2021). The *Leptoreodon* basioccipital has this median groove, although we could not determine if it extends onto the basisphen-

oid. Like *Protoceras*, *Leptoreodon* also has a bilateral groove extending rostrally from the base of the occipital condyles (Scott 1895, 1940; Robson et al. 2021).

Derived protoceratids, including *Protoceras*, *Syndyoceras*, and *Synthetoceras*, have a robust basioccipital that extends below the rest of the basicranium (Joeckel and Stavas 1996; Robson et al. 2021). The shape and cortical thickening of the bone are easily discernible from CT scans (Joeckel and Stavas 1996; Robson et al. 2021). Conversely, the basicranium of *Leptoreodon* is quite thin with little cortical bone and no ventral expansion. Norris (2000) described the basioccipital of *Leptotragulus* as being robust but, based on his illustrations, the bone does not appear to be ventrally expanded. It is likely that an enlarged basioccipital is the derived condition of protoceratids, perhaps associated with the development of cranial ornamentation.

The position of the basicapsular groove, which carries the inferior petrosal venous sinus in life (Joeckel and Stavas 1996), significantly differs between *Leptoreodon* and more derived protoceratids. *Syndyoceras* has a basicapsular groove solely on the basioccipital, a morphology not known to be present in any other artiodactyl (Joeckel and Stavas 1996). *Protoceras*, which is less derived than *Syndyoceras*, has a basicapsular groove that is predominately located on the basioccipital but includes a small contribution from the petrosal (Robson et al. 2021). *Leptotragulus* has a basicapsular groove on the petrosal but it is not known whether the basioccipital carries a complimentary groove (Norris 2000). Robson et al. (2021) suggested that *Protoceras* reflects a transitional morphology between the ancestral protoceratid condition and the derived condition observed in *Syndyoceras*. This inference is greatly supported by the morphology of *Leptoreodon*. The petrosal of *Leptoreodon* carries a deep basicapsular groove and, although the basioccipital forms the ventral border of the groove, there is no complimentary basicapsular groove on the basioccipital. This strongly suggests that the migration of a basicapsular groove on the basioccipital is a derived condition within the family. Indeed, the basicapsular groove morphology of *Leptoreodon* somewhat resembles that of a camelid, albeit without a petrosal ventromedial flange and without any contribution from the ectotympanic (Joeckel and Stavas 1996; Norris 1999; Robson et al. 2021).

Basisphenoid

The basisphenoid of *Leptoreodon* is typical of protoceratids (Scott 1895, 1940; Joeckel and Stavas 1996; Norris 2000; Robson et al. 2021), although damage to the medial portion of the bone means that some features cannot be observed on SDSNH 47878. The foramina observed on the specimen match descriptions of other *Leptotragulus* specimens, excepting the presence of a sphenoidal emissary

foramen, a small foramen that is known to exhibit intraspecific variation (Scott 1899).

Body mass and agility scores

Both body mass predictive equations provided similar body mass estimates for *Leptoreodon*. These estimates are comparable to those of similar sized artiodactyls, such as *Leptomeryx* (Damuth 1990). We used both mass estimates to predict agility scores. Agility scores are unitless values ranging from 1 to 6, with higher values indicating a greater amount of agility (Spoor et al. 2007). Of the extant artiodactyls that have been studied, species have agility scores between 2.53 (*Sus scrofa*) and 3.37 (*Gazella bennetti*) (Silcox et al. 2009). The agility scores of *Leptoreodon* are slightly lower than those of *Protoceras*, but they have overlapping ranges. The agility scores of *Protoceras* are only based on the anterior semicircular canal, but this does not hinder the comparison. *Protoceras* has values of 3.00 and 3.29 (depending on body mass; Robson et al. 2021). The equivalent anterior semicircular canal scores of *Leptoreodon* are 2.97 and 3.03. When all semicircular canals are considered, *Leptoreodon* has values ranging from 2.72 to 3.09. These values suggest that *Leptoreodon* was less cursorial than *Protoceras* but still fairly agile, similar to *Ovis aries* (Spoor et al. 2007: supplemental information), and these data are an additional line of evidence that protoceratids became more cursorial over time.

Phylogenetic relationships of *Leptoreodon* and *Leptotragulus*

An evolutionary relationship between *Leptoreodon*, *Leptotragulus*, and *Protoceras* has frequently been hypothesized, and there has been little debate as to whether *Leptoreodon* and *Leptotragulus* are related to each other, or to derived protoceratids (Scott 1899; Peterson 1919; Gazin 1955; Patton and Taylor 1973; Golz 1976). *Leptoreodon* and *Leptotragulus* are morphologically indistinguishable apart from differences in the p4 and, to a lesser extent, the p3; *Leptotragulus* has a p4 with a weaker metaconid, a more sharply flexed anterior crest, and a stronger parastylid (Gazin 1955). Both genera are similar to *Protoceras* in having a strong metaconid on p4, strong lingual cingula on the upper molars, and precocial selenodonty (Wilson 1974). To our knowledge, the placement of *Leptoreodon* and *Leptotragulus* within the Protoceratidae has been upheld in the published literature since the initial referral by Wilson in 1974 (Golz 1976; Black 1978; Prothero 1998; Norris 2000; Ludtke and Prothero 2004; Prothero and Ludtke 2007).

Until now, the dental characters identified by Gazin (1955) were the only known differences between *Leptoreodon* and *Leptotragulus*. Aside from a few notable

exceptions, the basicranial morphology of the two genera is also quite similar. The only known differences are found in the petrosal morphology—*Leptoreodon* has a deep subarcuate fossa and a dorsal process on the epitympanic wing, whereas *Leptotragulus* has a shallow subarcuate fossa and a rounded epitympanic wing. *Protoceras* also has a shallow subarcuate fossa but, like *Leptoreodon*, *Protoceras* has a dorsal process on the epitympanic wing. The deep subarcuate fossa of *Leptoreodon* is similar to that of basal camelids (Whitmore 1953; O’Leary 2010), but *Leptoreodon* has never been referred to the Camelidae. Differences in subarcuate fossa morphology are known to occur within artiodactyl families (O’Leary 2010), so the presence of a deep subarcuate fossa in *Leptoreodon* is not without precedent.

The basicranial morphologies of *Leptoreodon*, *Leptotragulus*, and derived protoceratids such as *Protoceras* do differ. Differences that may be phylogenetically significant, such as the shape of the subarcuate fossa, have already been discussed in detail. Other differences, such as the presence of a tegmen tympani fossa and a mastoid process in *Protoceras*, are most likely derived within the Protoceratidae. The only other identifiable basicranial distinction is that *Leptoreodon* has a pneumatized postglenoid process whereas *Protoceras* has a solid one. Given these data, we concur with the prevailing hypothesis that *Leptoreodon* and *Leptotragulus* are basal protoceratids, but we recognize that this hypothesis may need to be re-visited in the future.

Many systematics discussions have focused on competing hypotheses about the relationships of the Protoceratidae to the Ruminantia or the Tylopoda (Scott 1899; Peterson 1919; Gazin 1955). The petrosal morphology of *Leptotragulus*, *Protoceras*, and *Syndyoceras* has supported the hypothesis that protoceratids are closely related to the Ruminantia; all three genera have a shallow subarcuate fossa and lack a mastoid fossa, a morphology similar to that of pecoran ruminants (Joeckel and Stavas 1996; Norris 2000; O’Leary 2010; Robson et al. 2021). Conversely, most tylopods have a deep subarcuate fossa with a mastoid fossa (Whitmore 1953; Joeckel and Stavas 1996; Norris 1999; O’Leary 2010), a morphology similar to that of *Leptoreodon*. This shared morphology supports the hypothesis that protoceratids are closely related to (or are members of) the Tylopoda. However, some basal ruminants, such as *Leptomeryx*, have a deep subarcuate fossa (Whitmore 1953; Webb and Taylor 1980; O’Leary 2010), and the basal ruminant *Hypisodus* also has a mastoid fossa (Theodor 2010). It is possible that protoceratids and ruminants independently reduced the subarcuate fossa. If this is the case, the morphology of *Leptoreodon* does not support one hypothesized relationship over the other.

Other morphological features, such as the position of the basicapsular groove, are uninformative because there are

few published descriptions of these features in basal ruminants. For example, the basicapsular groove of *Leptoreodon* is primarily located on the petrosal, as it is in tylopods, but the petrosal of *Leptoreodon* lacks the ventromedial flange that roofs the basicapsular groove in tylopods (Joeckel and Stavas 1996). Basal ruminants also carry a basicapsular groove on their petrosal (Webb and Taylor 1980; O’Leary 2010), but the extent of this association is not known, so it cannot be determined whether the morphology of *Leptoreodon* is more similar to that of a tylopod or a basal ruminant.

CONCLUSIONS

Leptoreodon serves as a cautionary tale for morphology-based phylogenetic systematics. In many respects, the basicranial morphology of *Leptoreodon* is similar to that of other protoceratids. However, there are morphological differences, some of which may have great phylogenetic significance. Protoceratids and ruminants have been proposed to have a close evolutionary relationship because the two clades have basicranial similarities. This assessment has been predominately based on three protoceratid genera: *Leptotragulus*, *Protoceras*, and *Syndyoceras*. Of these, the internal basicranial morphology is only known from *Protoceras* and *Syndyoceras*, both of which are relatively derived taxa. The description of the basicranium of *Leptoreodon*—particularly the internal morphology—has demonstrated that basicranial features, including the morphology of the subarcuate fossa and the basicapsular groove, have greatly changed during protoceratid evolution. Yet, phylogenetic inferences have been primarily based on derived taxa that do not necessarily retain the ancestral morphology. As demonstrated by *Leptotragulus* and *Leptoreodon*, there is also morphological variation among basal protoceratids, indicating the value of examining several closely related taxa. We do not claim that the internal basicranial morphology of *Leptoreodon* overturns previous hypothesis of protoceratid evolutionary relationships. We merely suggest that such hypotheses should be re-evaluated considering these new data, and we caution against the inclusion of only highly derived taxa in future phylogenetic analyses.

ACKNOWLEDGEMENTS

We thank the San Diego Natural History Museum for loaning us SDSNH 47878 for scanning; T. Deméré and K. Randall were instrumental in this loan. We acknowledge that the specimen used in this study was collected on the ancestral lands of the Kumeyaay people. We also thank S. Cote and two anonymous reviewers for providing feedback on our manuscript. SVR acknowledges funding from the University of Calgary Faculty of Graduate Studies Eyes

High Doctoral Recruitment Scholarship, JAL acknowledges funding from the Systematics Research Fund through the Systematics Association, and JMT acknowledges funding from the Natural Sciences and Engineering Research Council of Canada (NSERC) Discovery Grants program.

LITERATURE CITED

- Black, C.C. 1978. Paleontology and geology of the Badwater Creek area, central Wyoming. Part 14: the artiodactyls. *Annals of the Carnegie Museum* 47:223–259.
- Colbert, E.H. 1941. The osteology and relationships of *Archaeomeryx*, an ancestral ruminant. *American Museum Novitates* 1135:1–24.
- Costeur, L. 2014. The petrosal bone and inner ear of *Micromeryx flourensianus* (Artiodactyla, Moschidae) and inferred potential for ruminant phylogenetics. *Zitteliana Reihe B: Abhandlungen Der Bayerischen Staatssammlung Fur Palaontologie Und Geologie* 32:99–114.
- Damuth, J. 1990. Problems in estimating body masses of archaic ungulates using dental measurements; pp. 229–253 in J. Damuth and B.J. MacFadden (eds.), *Body Size in Mammalian Paleobiology: Estimation and Biological Implications*. Cambridge University Press, Canada.
- Danilo, L., J. Remy, M. Vianey-Liaud, S. Mérigeaud, and F. Lihoreau. 2015. Intraspecific variation of endocranial structures in extant *Equus*: a prelude to endocranial studies in fossil equoids. *Journal of Mammalian Evolution* 22:561–582.
- Dechaseaux, C. 1969. Moulages endocraniens d'artiodactyles primitifs – essai sur l'histoire du néopallium. *Annales de Paléontologie* 55:195–248.
- Ekdale, E.G. 2009. Variation within the bony labyrinth of mammals. PhD dissertation, The University of Texas, Austin, TX, USA. 456 pp.
- Ekdale, E.G. 2013. Comparative anatomy of the bony labyrinth (inner ear) of placental mammals. *PLoS ONE* 8:27–28.
- Gazin, C.L. 1955. A review of the upper Eocene Artiodactyla of North America. *Smithsonian Miscellaneous Collections* 128:1–96.
- Gentry, A.W., and J.J. Hooker. 1988. The phylogeny of the Artiodactyla; pp. 235–272 in M.J. Benton (ed.), *The Phylogeny and Classification of the Tetrapods, Volume 2: Mammals*. Clarendon Press, Oxford.
- Golz, D.J. 1976. Eocene Artiodactyla of southern California. *Natural History Museum of Los Angeles County Science Bulletin* 26:1–85.
- Janis, C.M. 1990. Correlation of cranial and dental variables with body size in ungulates and macropodoids; pp. 255–300 in J. Damuth and B.J. MacFadden (eds.), *Body Size in Mammalian Paleobiology: Estimation and Biological Implications*. Cambridge University Press, Canada.
- Joekel, R.M., and J.M. Stavas. 1996. Basicranial anatomy of *Syndyoceras cooki* (Artiodactyla, Protoceratidae) and the need for a reappraisal of tylopod relationships. *Journal of Vertebrate Paleontology* 16:320–327.
- Kelly, T.S. 1990. Biostratigraphy of Uintan and Duchesnean land mammal assemblages from the middle member of the Sespe Formation, Simi Valley, California. *Natural History Museum of Los Angeles County, Contributions in Sciences* 419:1–42.
- Ludtke, J.A., and D.R. Prothero. 2004. Taxonomic revision of the middle Eocene (Uintan–Duchesnean) protoceratid *Leptoreodon* (Mammalia: Artiodactyla). *New Mexico Museum of Natural History and Science Bulletin* 26:101–111.
- Marsh, O.C. 1891. A horned artiodactyle (*Protoceras celer*) from the Miocene. *American Journal of Science* 41:5a–6a.
- Matthew, W.D. 1899. A provisional classification of the freshwater Tertiary of the West. *Bulletin of the American Museum of Natural History* 12:19–75.
- Matthew, W.D. 1905. Notice of two new genera of mammals from the Oligocene of South Dakota. *Bulletin of the American Museum of Natural History* 21:21–26.
- Mennecart, B., and L. Costeur. 2016a. A *Dorcatherium* (Mammalia, Ruminantia, middle Miocene) petrosal bone and the tragulid ear region. *Journal of Vertebrate Paleontology* 36:e1211665.
- Mennecart, B., and L. Costeur. 2016b. Shape variation and ontogeny of the ruminant bony labyrinth, an example in Tragulidae. *Journal of Anatomy* 229:422–435.
- Mennecart, B., G.E. Rössner, G. Métails, D. DeMiguel, G. Schulz, B. Müller, and L. Costeur. 2016. The petrosal bone and bony labyrinth of early to middle Miocene European deer (Mammalia, Cervidae) reveal their phylogeny. *Journal of Morphology* 277:1329–1338.
- Norris, C.A. 1999. The cranium of *Bunomeryx* (Artiodactyla: Homacodontidae) from the Upper Eocene Uinta deposits of Utah and its implications for tylopod systematics. *Journal of Vertebrate Paleontology* 19:742–751.
- Norris, C.A. 2000. The cranium of *Leptotragulus*, a hornless protoceratid (Artiodactyla: Protoceratidae) from the Middle Eocene of North America. *Journal of Vertebrate Paleontology* 20:341–348.
- O'Leary, M.A. 2010. An anatomical and phylogenetic study of the osteology of the petrosal of extant and extinct artiodactylans (Mammalia) and relatives. *Bulletin of the American Museum of Natural History* 335:1–206.
- O'Leary, M.A. 2016. Comparative basicranial anatomy of extant terrestrial and semiaquatic Artiodactyla. *Bulletin of the American Museum of Natural History* 409:1–55.
- Orliac, M.J., and M.A. O'Leary. 2014. Comparative anatomy of the petrosal bone of dichobunoids, early members of Artiodactylamorpha (Mammalia). *Journal of Mammalian Evolution* 21:299–320.
- Orliac, M.J., J. Benoit, and M. O'Leary. 2012. The inner ear of *Diacodexis*, the oldest artiodactyl mammal. *Journal of Anatomy* 221:417–426.
- Orliac, M.J., R. Araújo, and F. Lihoreau. 2017. The petrosal and bony labyrinth of *Diplobune minor*, an enigmatic Artiodactyla from the Oligocene of Western Europe. *Journal of Morphology* 278:1168–1184.

- Osborn, H.F., and J.L. Wortman. 1892. Characters of *Protoceras* (Marsh), the new artiodactyl from the Lower Miocene. *Bulletin of the American Museum of Natural History* 18:351–371.
- Patton, T.H., and B.E. Taylor. 1971. The Synthetoceratinae (Mammalia, Tylopoda, Protoceratidae). *Bulletin of the American Museum of Natural History* 145:123–218.
- Patton, T.H., and B.E. Taylor. 1973. The Protoceratinae (Mammalia, Tylopoda, Protoceratidae) and the systematics of the Protoceratidae. *Bulletin of the American Museum of Natural History* 150:351–413.
- Peterson, O.A. 1919. Report upon the material discovered in the upper Eocene of the Uinta Basin by Earl Douglas in the years 1908-1909, and by O.A. Peterson in 1912. *Annals of the Carnegie Museum* 12:40–168.
- Prothero, D.R. 1998. Protoceratidae; pp. 431–438 in C.M. Janis, K.M. Scott, and L.L. Jacobs (eds.), *Evolution of Tertiary Mammals of North America, Volume 1, Terrestrial Carnivores, Ungulates, and Ungulate-like Mammals*. Cambridge University Press, Cambridge.
- Prothero, D.R., and J.A. Ludtke. 2007. Family Protoceratidae; pp. 169–176 in D.R. Prothero and S.E. Foss (eds.), *The Evolution of Artiodactyls*. The Johns Hopkins University Press, Baltimore.
- Robson, S.V., B. Seale, and J.M. Theodor. 2021. The petrosal and basicranial morphology of *Protoceras celer*. *PLoS ONE* 16: e0251832.
- Scott, W.B. 1895. The osteology and relationships of *Protoceras*. *Journal of Morphology* 2:303–363.
- Scott, W.B. 1898. Preliminary note on the selenodont artiodactyls of the Uinta Formation. *Proceedings of the American Philosophical Society* 37:73–81.
- Scott, W.B. 1899. The selenodont artiodactyls of the Uinta Eocene. *Transactions of the Wagner Free Institute of Science* 6:1–120.
- Scott, W.B. 1940. The mammalian fauna of the White River Oligocene: Part IV. Artiodactyla. *Transactions of the American Philosophical Society* 28:363–746.
- Silcox, M.T., J.I. Bloch, D.M. Boyer, M. Godinot, T.M. Ryan, F. Spoor, and A. Walker. 2009. Semicircular canal system in early primates. *Journal of Human Evolution* 56:315–327.
- Simpson, G.G. 1945. The principles of classification and a classification of mammals. *Bulletin of the American Museum of Natural History* 85:1–350.
- Spoor, F., T. Garland, G. Krovitz, T.M. Ryan, M.T. Silcox, and A. Walker. 2007. The primate semicircular canal system and locomotion. *PNAS* 104:10808–10812.
- Stirton, R. 1967. Relationships of the Protoceratid Artiodactyls and Description of a New Genus. University of California Press, Berkeley, 44 pp.
- Stirton, R.A. 1944. Comments on the relationships of the cervoid family Palaeomerycidae. *American Journal of Science* 242:633–655.
- Stock, C. 1936. *Hesperomeryx*, a new artiodactyl from the Sespe Eocene, California. *National Academy of Sciences Proceedings* 22:177–182.
- Theodor, J. 2010. Morphology of the auditory region of *Hypisodus minimus*: implications for the evolution of the mastoid fossa of artiodactyls. 70th Anniversary Meeting Society of Vertebrate Paleontology 174A.
- Webb, S.D. 1981. *Kyptoceras amatorum*, new genus and species from the Pliocene of Florida, the last protoceratid artiodactyl. *Journal of Vertebrate Paleontology* 1:357–365.
- Webb, S.D., and E.B. Taylor. 1980. The phylogeny of hornless ruminants and a description of the cranium of *Archaeomeryx*. *Bulletin of the American Museum of Natural History* 167:117–158.
- Whitmore, F.C. 1953. Cranial morphology of some Oligocene Artiodactyla. United States Geological Survey Professional Paper 243-H:117–160.
- Wilson, J.A. 1974. Early Tertiary vertebrate faunas, Vieja Group and Buck Hill Group, Trans-Pecos Texas: Protoceratidae, Camelidae, Hypertragulidae. *Texas Memorial Museum, University of Texas at Austin* 23:1–34.
- Wilson, J.A. 1984. Vertebrate faunas 49 to 36 million years ago and additions to the species of *Leptoreodon* (Mammalia: Artiodactyla) found in Texas. *Journal of Vertebrate Paleontology* 4:1–4.
- Wortman, J.L. 1898. The extinct Camelidae of North America and some associated forms. *The Bulletin of the AMNH* 10:1–141.